Journal of Biomechanics 204 (2026) 113346

Contents lists available at ScienceDirect

Journal of Biomechanics

journal homepage: www.elsevier.com/locate/jbiomech

Enhancing fear of re-injury classification after ACL reconstruction by integrating biomechanical and electromyography data using multimodal machine learning methods

Abdolamir Karbalaie [a], Adam Grinberg [a], Andrew Strong [a], Helena Grip [b], Kalle Prorok [a], Charlotte K. Häger [a,b,1,*], Tomas Nordström [c,1]

[a] Dept of Community Medicine and Rehabilitation, Umeå University, Sweden
[b] Dept of Diagnostics and Intervention, Umeå University, Sweden
[c] Dept of Applied Physics and Electronics, Umeå University, Sweden

ARTICLE INFO

Keywords:
EMG
Kinematics
Kinetics
Side hop
Artificial intelligence
Feature extraction

ABSTRACT

Fear of re-injury after anterior cruciate ligament (ACL) rupture often hinders return-to-sport and has been linked to movement patterns associated with increased injury risk. Identifying fearful individuals is thus critical. Self-reported questionnaires are commonly used but may be affected by underreporting in sporting and clinical contexts. We aimed to classify individuals with ACL reconstruction (ACLR) into HIGH-FEAR and LOW-FEAR groups, using machine learning (ML) models trained on unimodal or multimodal time-series movement data from side hop landings. Seventy-two participants (median: 13.0 months post-ACLR; interquartile range: 15.8 months) were dichotomized into HIGH-FEAR/LOW-FEAR groups using a single item (statement 9) from the Tampa Scale for Kinesiophobia. Participants performed one-leg standardized rebound side hops while kinematics and kinetics were recorded using 3D motion capture and force plates, respectively, and electromyography (EMG) was registered from flexor and extensor thigh muscles. We extracted time-series features from each modality and ten ML algorithms were trained and evaluated using leave-one-participant-out and grouped 3-fold cross-validation. Integrating kinematic/kinetic and EMG data improved classification accuracy compared to single modality datasets. The extreme gradient boosting model achieved the highest accuracy for fused data (86%) using the top 40 ranked features, including trunk tilt, pelvic obliquity, knee rotation, and flexor and extensor muscle activations. Kinematic/kinetic data alone achieved 83% accuracy per participant, while EMG data alone yielded 85%. This study demonstrates the potential of integrating different movement-related data to enhance the accuracy of ML models in classifying fear of re-injury post-ACLR, supporting identification of patterns associated with fear and guiding treatment.

1. Introduction

Fear of re-injury is a major psychological barrier preventing many athletes following rupture of the anterior cruciate ligament from returning to their pre-injury activity levels (Ardern et al., 2011; Hamdan et al., 2025). Despite advances in surgical techniques and rehabilitation protocols following ACL reconstruction (ACLR), return-to-sport rates remain suboptimal, with 44–65% of individuals failing to resume competitive sports—largely due to psychological barriers (Ardern et al., 2014; Ardern et al., 2011; Du et al., 2022; Hamdan et al., 2025). Although some interventions have shown effective in reducing re-lapse/re-injury worries in e.g., low back pain (Woods and Asmundson, 2008), similar benefits have not been observed in individuals who have had ACLR (Baez et al., 2021), possibly due to limitations in assessment methods.

Commonly used self-reported questionnaires may be inadequate in real-world sporting and clinical contexts, as athletes often underreport their insecurities to protect their image (Heil, 2000) or avoid revealing psychological barriers delaying return-to-sport clearance (Grossbard et al., 2007; King and Bruner, 2000; Wiechman et al., 2000). Fear of re-

* Corresponding author.
E-mail address: charlotte.hager@umu.se (C.K. Häger).
[1] The last authorship is shared between Charlotte K. Häger and Tomas Nordström.

https://doi.org/10.1016/j.jbiomech.2026.113346
Accepted 4 May 2026
Available online 6 May 2026

injury may however be manifested in aberrant movement patterns such as leg stiffening during jump-landings (Trigsted et al., 2018) and side-hops (Markström et al., 2022a). In the latter, individuals with high self-reported fear demonstrated greater hamstring activation and increased anteroposterior muscle co-contraction compared to those with low fear or uninjured controls. Identifying individuals with movement patterns associated with fear of re-injury may therefore complement self-reported questionnaires. This seems particularly important before resuming physical activity and would be a critical step towards tailored rehabilitation efforts.

Laboratory motion capture systems generate large multimodal datasets, including biomechanical measures and electromyography (EMG). Kinematic (movement-related) and kinetic (force-related) analyses offer detailed information on joint angles, moments, and ground reaction forces, while EMG captures neuromuscular activation patterns not observable from kinematics or kinetics alone. Machine learning (ML) techniques offer a promising approach to integrate multimodal data to better understand the consequences of fear of re-injury. In this context, we recently proposed a deep learning approach using kinematic and kinetic data to classify individuals as having high or low fear following ACLR (Karbalaie et al., 2025). Although laboratory-based measurements allow detailed assessment of these features, general inaccessibility and associated costs limit their broader applicability (Johnson et al., 2019). Portable sensors such as wearable EMG devices provide more accessible alternatives in clinical or field settings (Krishnakumar et al., 2024). It remains, however, unclear whether EMG alone is sufficient or whether combining multiple signal types would further improve classification accuracy. Recent work supports acquiring complementary information from wearable-derived biomechanical and muscle-force estimates (Moghadam et al., 2023).

The present study evaluated the use of EMG or biomechanical data separately, as well as their combination, acquired during side hops performed in a laboratory setting, in machine learning (ML) models for classifying individuals post-ACLR as HIGH-FEAR or LOW-FEAR based on questionnaire-defined fear categories. Specific aims were to: (1) evaluate the classification performance of various ML models, related to fear of re-injury, based on single-modality biomechanical or EMG data separately, and (2) determine whether multimodal integration enhances classification performance compared to single-modality approaches. We hypothesized that while single-modality data streams would yield high classification accuracy, multimodal ML models would further enhance performance. Reporting follows TRIPOD-AI (Checklist; Supplementary S1).

2. Methods

2.1. Study design

This cross-sectional study was approved by the regional ethical review board in Umeå, Sweden (Project No. 2015/67–31; 2021–03860). Participants provided informed consent, and the study was conducted in accordance with the Declaration of Helsinki.

2.2. Participants

Participants were recruited using convenience sampling through orthopedic and sports medicine clinics, local sports clubs, and university campus advertisements. Eligibility criteria included ages 15–35 years, ability to perform single-leg hops, unilateral ACLR with a hamstring autograft within the past five years, and absence of other injuries (except concomitant meniscal tear) affecting hop performance. Of the 88 participants initially recruited, ten were excluded due to incomplete kinematic data and six to incomplete EMG recordings. The final sample consisted of 72 participants (Table 1). This convenience sample, although including a higher proportion of females (50/72), is consistent with an elevated ACL injury risk reported in young female athletes (Hewett et al., 2005).

Table 1
Demographics and patient-reported outcome measures for all participants combined and when categorized by fear of re-injury.

Characteristics	Total	LOW-FEAR	HIGH-FEAR
Male:Female, n[a]	22:50	11:25	11:25
Age, years, Mean (SD)	24.5 (4.5)	24.7 (4.7)	24.4 (4.3)
Months since surgery, Median (IQR)	13.0 (15.8)	13.4 (21.7)	13.0 (11.3)
Anthropometric measurements, Mean (SD)			
Body height, cm	172.2 (8.2)	172.0 (8.7)	172.4 (7.7)
Body mass, kg	71.2 (10.6)	71.1 (11.4)	71.3 (9.8)
Body mass index, kg/m^2	23.9 (2.4)	24.0 (2.8)	23.9 (2.1)
Patient-Reported Outcome Measures, Median (IQR)			
Tampa Scale of Kinesiophobia, 17–68	31.0 (8.8)	29.0 (7.5) *	34.0 (6.8)
IKDC2000, % of maximum	79.9 (13.2)	85.5 (10.9) *	77.0 (12.1)
KOOS, % of maximum			
Symptoms	82.1 (21.5)	87.5 (21.4) *	73.2 (20.5)
Pain	91.7 (11.1)	94.4 (8.3) *	88.9 (10.4)
Activities of Daily Living	100.0 (1.5)	100.0 (1.5) *	98.5 (2.9)
Sports/Recreation	80.0 (23.8)	90.0 (15.0) *	70.0 (23.8)
Quality of Life	62.5 (23.4)	71.9 (18.8) *	56.3 (17.2)
Lysholm Score, 1–100	89.0 (11.8)	90.5 (11.5) *	88.0 (11.5)
Tegner Activity Scale, 0–10			
Pre-injury score	9.0 (2.0)	9.0 (2.0)	9.0 (2.0)
Current score	6.5 (3.5)	6.5 (4.8)	6.5 (2.0)

* Statistically significant difference between LOW-FEAR and HIGH-FEAR groups ($p < 0.05$).
[a]Eight participants have two test sessions included in the main data analysis but only data related to their first test session have been included to calculate group characteristics.
IKDC: International Knee Documentation Committee Subjective Knee Form; IQR: interquartile range; KOOS: Knee injury and Osteoarthritis Outcome Score; SD: standard deviation.
Note: The Tampa Scale of Kinesiophobia (TSK) assesses pain-related fear of movement and re-injury, ranging from 17 to 68, with higher scores indicating greater levels of kinesiophobia. The Lysholm Knee Score evaluates knee function on a scale from 0 to 100, where higher scores reflect better functionality. The Tegner Activity Scale quantifies knee-specific physical activity levels from 0 to 10, with 0 representing minimal activity (e.g., sedentary lifestyle) and 10 denoting participation in elite-level, knee-intensive sports such as soccer or ice hockey.

After recruitment and data-quality screening, participants were classified as HIGH-FEAR or LOW-FEAR using statement 9 of the Tampa Scale of Kinesiophobia (TSK-17): '*I am afraid that I might injure myself accidentally*' (Markström et al., 2022a). Responses of 'Agree' or 'Strongly agree' defined HIGH-FEAR, and other responses defined LOW-FEAR. Notably, this questionnaire-based classification was used as a pragmatic reference for group definition rather than as a gold standard assessment of fear of re-injury. In clinical and sport contexts self-reported fear may be biased or attenuated (King and Bruner, 2000), but remains an accepted approach for operationalizing psychological constructs under controlled experimental conditions assuring confidentiality and without consequences of participants' responses. The HIGH-FEAR and LOW-FEAR categorization thus seems a valid group labeling. The final analytic sample comprised 36 participants per group with identical sex distribution (11:25 in each group).

Data from this cohort have been included in prior analyses focusing on standard statistical comparisons in a smaller subset (n = 38 (Markström et al., 2022a)) and biomechanical-only deep learning

analysis (n = 60 (Karbalaie et al., 2025)). The present study differs by analyzing an expanded cohort (n = 72) and uniquely applying multimodal machine learning to evaluate the specific classification utility of EMG separately and while integrated with biomechanics.

2.3. Data collection procedures

2.3.1. Test procedures and equipment

Participants performed the one-leg standardized rebound side hop (SRSH) test (Fig. 1), previously described in detail and used to differentiate between HIGH-FEAR and LOW-FEAR individuals with ACLR based on landing biomechanics (Markström et al., 2022a). The SRSH involves repeated single-leg landings under standardized conditions that are relevant to post-ACLR movement control. Testing was conducted at the U-Motion Laboratory, Umeå University, Sweden. Fifty-six retroreflective markers were placed on anatomical landmarks of the body. An 8-camera 3D motion capture system (240 Hz, Oqus 300, Qualisys AB, Sweden) synchronized with two force platforms (1200 Hz, Kistler 9286AA, Switzerland) registered kinematics and kinetics, respectively. Surface EMG data were simultaneously recorded at 1500 Hz using a direct transmission system (TeleMyo 542 DTS, Noraxon USA Inc.). Electrodes were placed according to SENIAM guidelines (Hermens et al., 1999) over the biceps femoris (BF), semitendinosus (ST), vastus medialis (VM), and vastus lateralis (VL) muscles. Skin preparation involved

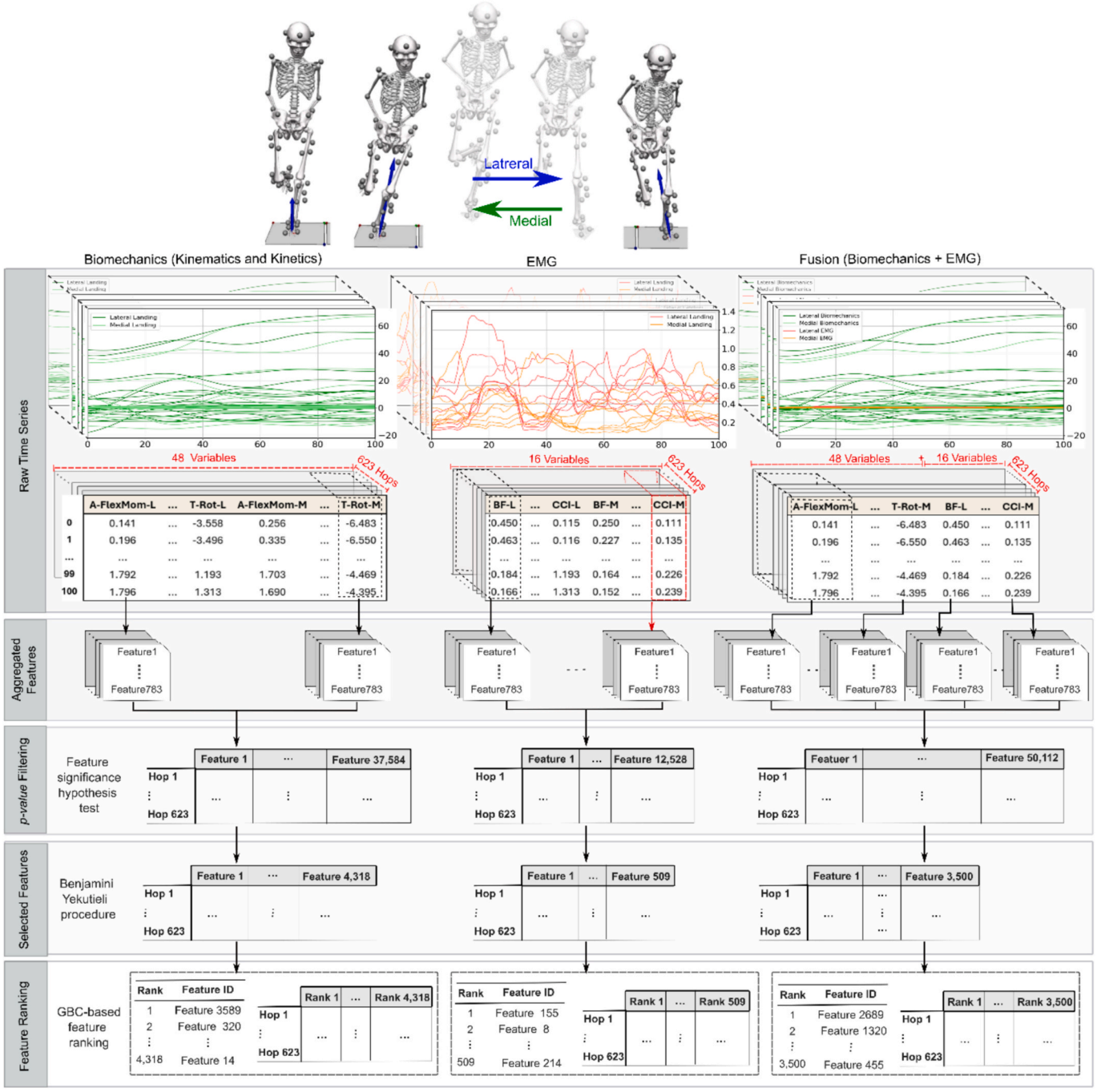

Fig. 1. Feature Extraction and Selection Process using tsfresh. **Note:** GBC = Gradient Boosting Classifier; A-FlexMom = Ankle Flexion/Extension Moment in Lateral; T-Rot = Trunk Rotation in Lateral; BF = Biceps Femoris; CCI = Co-Contraction Index; L = Lateral; M = Medial; tsfresh = time series feature extraction on basis of scalable hypothesis.

shaving, scrubbing, and cleaning with isopropyl alcohol to reduce impedance. Electrodes were positioned with a 20 mm inter-electrode distance.

Participants completed ten hops per leg to the side and immediately back again. Standardized hop distance was set at 10% of the body height of each participant. Hops were excluded if participants hopped noticeably shorter or longer than the standardized distance, adjusted their feet after initial ground contact, lost balance within three seconds, or released the rope they held with both hands behind their back. Raw marker and analog data were recorded with Qualisys Track Manager (v2019.3, Qualisys).

2.4. Data processing

2.4.1. Signal preprocessing of biomechanical and EMG data

Marker trajectories were tracked using Qualisys Track Manager (v. 2019.3) and exported to Visual3D (v. 5.02.30; C-Motion) for kinematic and kinetic processing. Data were filtered using a critically damped zero-lag digital low-pass filter set at 15 Hz to reduce noise and preserve signal integrity. An eight-segment, six–degrees-of-freedom kinematic model defined the trunk, pelvis, thigh, shank, and foot segments (see, e.g., (Markström et al., 2022a; Markström et al., 2022b; Markström et al., 2021)). Each segment was tracked by at least three markers, with rigid marker clusters used on the thighs. The distal and proximal ends of each segment were defined using markers placed on anatomical landmarks. Hip joint centers were determined with a functional joint-center method described by Schwartz and Rozumalski (Schwartz and Rozumalski, 2005), while knee and ankle joint centers were identified based on markers placed over the femoral epicondyles and malleoli, respectively. A Cardan XYZ rotation sequence was used to compute joint angles as the relative orientation between two adjacent segments. Joint kinetics were calculated via inverse dynamics using the resultant moments approach, with coordinate systems resolved in the reference segment's coordinate system (Markström et al., 2022b). All analyzed time-series were time-normalized using 3-rd order polynomial fitting interpolation to ensure consistent comparisons across participants and trials. Moments were normalized to body mass and expressed as external moments.

EMG signals were band-pass filtered (20 Hz–500 Hz) to remove low-frequency noise and high-frequency artifacts. A root mean square (RMS) moving window of 20 ms was then applied to smooth the signals. EMG amplitudes were normalized to the average peak amplitude during the landing phase to account for inter-participant variability in muscle activation levels.

The analysis focused on the landing phases (lateral and medial), defined as the intervals from initial ground contact to maximum knee flexion.

2.4.2. Outlier Detection and Removal

Outliers in EMG data were identified using an interquartile range (IQR) rule (Dekking et al., 2005), with peak EMG values flagged as outliers if they fell below $Q1 - 1.5 \times IQR$ or above $Q3 + 1.5 \times IQR$. Trials flagged as outliers were discarded. A total of six hops were identified as outliers and removed, ensuring that all participants retained at least five successful hops, resulting in a dataset of 623 (HIGH-FEAR = 301, LOW-FEAR = 322) valid hop trials.

3. Data analysis

3.1. Engineering of variables and feature extraction

3.1.1. Engineered EMG variables

To characterize neuromuscular activation patterns during dynamic landing tasks, we engineered EMG features from time-series signals recorded for flexor (BF, ST) and extensor (VL, VM) muscle groups. These features were computed for all 101 time points during the landing phase to capture temporal variation:

- **Flexor Average Activation:** $F_{\text{avg}}(t) = \frac{EMG_{\text{BF}}(t)+EMG_{\text{ST}}(t)}{2}$
- **Extensor Average Activation:** $E_{\text{avg}}(t) = \frac{EMG_{\text{VL}}(t)+EMG_{\text{VM}}(t)}{2}$
- **Co-contraction Ratio (CCR):** $CCR(t) = \frac{\min(F_{\text{avg}},E_{\text{avg}})}{\max(F_{\text{avg}},E_{\text{avg}})}$
- **Co-contraction Index (CCI):** $CCI(t) = \frac{F_{\text{avg}}(t)+E_{\text{avg}}(t)}{2} \times CCR(t)$

where t represents individual time steps within the series and EMG_{BF}, EMG_{ST}, EMG_{VL} and EMG_{VM} are the EMG signals recorded from the respective muscles. These time-resolved metrics reflect dynamic patterns of muscle co-activation and balance during landing.

3.2. Data categorization

To ensure clarity, we categorized the data as follows:

Variables: Time-normalized time-series data from joint angles, moments, and EMG signals.
Variable Engineering: EMG-derived variables (e.g., F_{avg}, E_{avg}, CCR, CCI).
Features: Higher-level features extracted from time-series variables using the time series feature extraction on basis of scalable hypothesis tests (tsfresh) library.

3.3. Feature extraction, selection and ranking

We used the tsfresh library (Christ et al., 2018) to extract time-series features from the biomechanical, EMG, and fused datasets. A significance-based filter ($p < 0.05$) was first applied. We then ranked the remaining features using Random Forest (RF), Extra Trees (ET), and Gradient Boosting Classifier (GBC) models to identify the most important predictors. The GBC model was selected for final ranking, and we progressively evaluated feature subsets (from 5 to 350) to find the optimal set for classification performance (Fig. 1) (Guyon and E.a., 2003; Saeys et al., 2007). Each model input feature is a scalar descriptor computed from the full time-normalized landing trajectory (101 time points) for a given variable and side (i.e., a variable × tsfresh feature-function pair), rather than a single event sample. Further details are in Supplementary Material S2–S3.

3.4. Data standardization

Features were standardized using scikit-learn's StandardScaler (zero mean, unit variance) fit on the training data within each fold and applied to the corresponding test data.

3.5. Classification models and validation

3.5.1. Machine learning algorithms

We evaluated ten supervised ML algorithms, including linear models (LR, Linear Discriminant Analysis (LDA), Quadratic Discriminant Analysis (QDA)), instance-based learning k-Nearest Neighbors (KNN), and ensemble/tree-based methods (RF, ET, GBC, AdaBoost (ADA), Extreme Gradient Boosting (XGB), and Light Gradient Boosting Machine (LGBM)) to capture both linear and non-linear relationships.

3.5.2. Hyperparameter tuning

Hyperparameters were tuned using nested cross-validation, with grid search applied in the inner loop on the biomechanical dataset. The resulting configurations were reused across EMG and fused datasets to preserve comparability and reduce computational overhead.

3.5.3. Cross-validation strategy

To rigorously evaluate model performance and reduce overfitting, a two-level cross-validation strategy was employed. In the outer loop,

leave-one-participant-out cross-validation (LOPOCV) was used, where each participant's data served exclusively as the test set in one-fold. This ensured participant-level independence between training and testing, enhancing generalizability (Lee and Lee, 2024; Palma Fraga et al., 2023).

Within each LOPOCV fold, the training set was further divided using grouped 3-fold cross-validation (GroupKFold-3). Each split contained unique participants to avoid data leakage between folds. This inner loop provided an unbiased internal validation and helped detect overfitting during model training, thereby improving the robustness of the final evaluation.

3.5.4. Feature importance calculation and visualization

To identify the most influential features for classifying HIGH-FEAR and LOW-FEAR individuals, feature importance scores were extracted from the top-performing models that inherently provide such measures. These scores were computed within each outer cross-validation fold and averaged across folds to reduce variability and yield a stable estimate of feature relevance.

The resulting unitless scores reflect each feature's relative contribution to model predictions. To enhance interpretability, feature names generated by the tsfresh library were simplified and grouped by biomechanical function and landing direction for biomechanical data, and by specific engineered metrics (e.g., CCI) for EMG data. Within each group, scores were averaged to generate aggregate importance values. These were visualized using grouped bar plots with refined labels to facilitate interpretation.

For details on ML algorithms, hyperparameter tuning, and feature importance calculation, see Supplementary Materials S2.

3.5.5. Evaluation metrics and performance analysis

Model performance was assessed at both hop and participant levels. At the hop level, each hop trial inherited the fear label of its participant (HIGH-FEAR/LOW-FEAR), and we computed accuracy (ACC), F1-score, and Matthews' correlation coefficient (MCC) to quantify trial-level discrimination. At the participant level, hop-level predictions were aggregated using majority voting: a participant was categorized as HIGH-FEAR if $\geq$ 50% of their hops were predicted as HIGH-FEAR; otherwise, LOW-FEAR. Participant-level performance was evaluated using accuracy, sensitivity, and specificity. Sensitivity was defined as the true-positive rate for HIGH-FEAR (TP/(TP + FN)), and specificity as the true-negative rate for LOW-FEAR (TN/(TN + FP)). Both were computed from the participant-level confusion matrix obtained by aggregating held-out predictions across the outer validation splits. This two-level evaluation links trial-level classification to the clinical objective of identifying individuals with fear of re-injury.

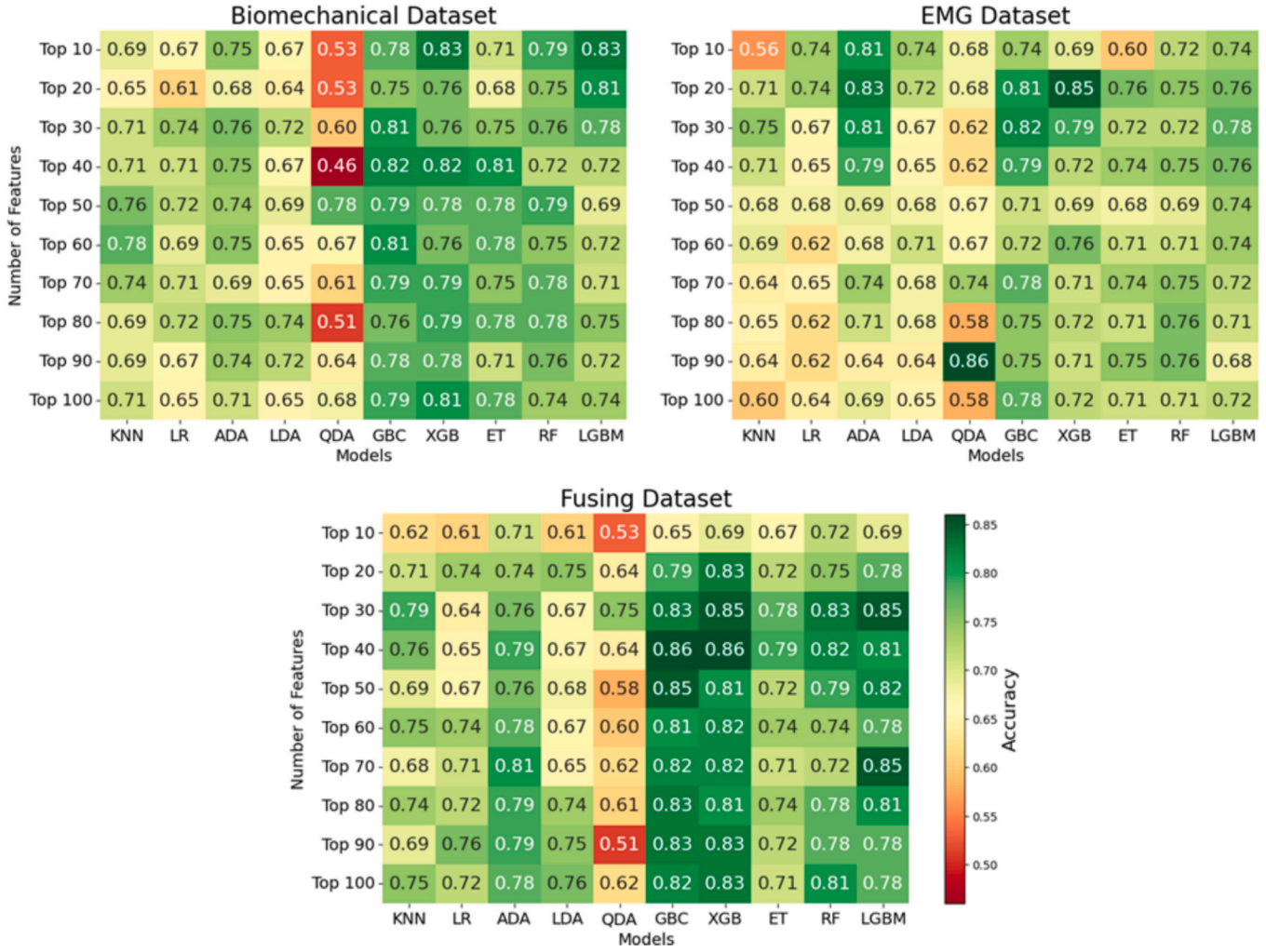

Fig. 2. Heatmaps of Classification Accuracy for Selected Features in Three Datasets ***Note:*** *KNN = K-Nearest Neighbors; LR = Logistic Regression; ADA = AdaBoost; LDA = Linear Discriminant Analysis; QDA = Quadratic Discriminant Analysis; GBC = Gradient Boosting Classifier; XGB = Extreme Gradient Boosting; ET = Extra Trees; RF = Random Forest; LGBM = Light Gradient Boosting Machine.* ***Color Scale:*** *Green indicates higher classification accuracy; red indicates lower accuracy.* (For interpretation of the references to colour in this figure legend, the reader is referred to the web version of this article.)

3.5.6. Model selection

All ten machine learning algorithms were evaluated systematically across multiple feature subset sizes, ranging from the top 5 to 350 features and across three data modalities: biomechanical, EMG, and fused datasets. Model selection was based on the consistency of classification performance across key evaluation metrics, robustness under both LOPOCV and GroupKFold-3, interpretability for potential clinical applications, and computational efficiency. Only the most performant and interpretable models are reported in the Results section.

3.5.7. Computational environment

Analyses used Python (scikit-learn, XGBoost, LightGBM). Computational details are provided in the Supplementary S3.

4. Results

4.1. Classification performance and optimal feature selection

Heatmaps (Fig. 2) show how accuracy changes as the number of selected features increases. Across all three data types, AdaBoost often matched or outperformed Logistic Regression, while Logistic Regression is kept as a simple linear baseline. For readability, Tables 2–3 report four selected models (LR, GBC, XGB, LGBM), and full results for all models and feature counts are provided in Supplementary Material S3.

For the biomechanical d*ataset*, both XGB and LGBM models achieved a maximum accuracy of 83% using the top 10 features. In the EMG dataset, QDA achieved the highest accuracy of 86% with the top 90 features. Among interpretable models, XGB had the highest accuracy of 85% using the top 20 features. For the *fused dataset*, XGB and GBC both reached the highest accuracy of 86% using the top 40 features.

4.2. Participant-level classification

The best models, XGB and GBC, showed high accuracy in earlier tests (Table 2) including accuracy, sensitivity, and specificity scores for the selected models across the biomechanical, EMG, and fused datasets. Results are shown for the top 10, 20, and 40 features.

4.3. Hop-level classification

Table 3 summarizes hop-level classification results generated using two cross-validation approaches**,** for selected models (LR, GBC, XGB, LGBM) across single modality and fused datasets, based on the top 10, 20, and 40 features. Notably, in the fused dataset using the top 40 features, XGB achieved the highest LOPOCV accuracy of 79%, with an F1-score of 78% and an MCC of 0.57. Similarly, GBC attained an LOPOCV accuracy of 77%, F1-score of 76%, and MCC of 0.54 with the same feature set. Across all models and feature sets, the mean absolute ACC difference between LOPOCV and GroupKFold-3 was 0.03 ± 0.02. For the fused XGB model using the Top-40 features, hop-level predictions were generally consistent within participants: 63.9% (46/72) of participants exhibited at most one deviating hop, whereas only 1.4% (1/72) showed near-balanced hop patterns. The full distribution of hop-level consistency across participants is reported in Supplementary Fig. S3.4 and Supplementary Table S3.

4.4. Feature importance analysis

Feature importance analysis using the top-performing XGB model (Fig. 3a-c) revealed key biomechanical and muscular discriminators between fear groups (full rankings available in Supplementary Material S4). As illustrated in Fig. 3a, the most influential tsfresh-derived features were computed from the pelvis obliquity, trunk tilt, and knee rotation trajectories, indicating that these variables contained the strongest discriminative signal between fear groups under the selected model. Muscle activation patterns, particularly the average activations of flexor and extensor muscle groups in the leg, played a critical role in classification (Fig. 3b). The balance between hamstring and quadriceps muscle activations was influential in distinguishing HIGH-FEAR and LOW-FEAR participants. For fused data, key features included lateral knee rotation, medial flexor average activation, and medial trunk tilt (Fig. 3c).

5. Discussion

This study evaluated ML models trained on biomechanical and EMG data separately (single-modality) and in combination (multimodal). Multimodal fusion consistently outperformed single-modality models, indicating that kinematic/kinetic signals and EMG capture complementary aspects of landing strategy linked to fear-of-re-injury after ACLR. Although the accuracy gain was modest relative to the best single-modality models, stability across validation, feature-ranking consistency, and improvements in secondary metrics (e.g., F1, MCC) support the added value of fusion.

Our findings align with and extend previous research documenting fear-related lower extremity biomechanics and muscle activation patterns following ACL reconstruction (Markström et al., 2022a; Trigsted et al., 2018). It should however be noted that these associations may depend on the choice of functional movement and muscle tested (Dudley et al., 2022). While our results suggest that fear of re-injury post-ACLR may be linked to interactions between mechanical alignment and neuromuscular control, given the cross-sectional design, the direction of this relationship cannot be determined.

5.1. Clinical relevance and methodological implications

Our study shows that subjectively defined fear groups differ in

Table 2
Participant-level classification performance across models and feature sets.

Data Type		Top 10			Top 20			Top 40		
Model		ACC	Sens	Spec	ACC	Sens	Spec	ACC	Sens	Spec
BiomecHanical	**LR**	0.67	0.67	0.67	0.61	0.61	0.61	0.71	0.71	0.69
	GBC	0.78	0.78	0.78	0.75	0.74	0.78	0.82	0.83	0.81
	XGB	**0.83**	**0.85**	0.81	0.76	0.74	0.81	0.82	0.81	0.83
	LGBM	**0.83**	0.83	0.83	0.81	0.81	0.81	0.72	0.71	0.75
EMG	**LR**	0.74	0.76	0.69	0.74	0.74	0.72	0.65	0.66	0.64
	GBC	0.74	0.72	0.78	0.81	0.78	0.86	0.79	0.76	0.86
	XGB	0.69	0.68	0.75	**0.85**	**0.82**	0.89	0.72	0.7	0.78
	LGBM	0.74	0.69	0.86	0.76	0.73	0.83	0.76	0.74	0.81
Fused	**LR**	0.61	0.61	0.64	0.74	0.7	0.83	0.65	0.65	0.67
	GBC	0.65	0.65	0.67	0.79	0.76	0.86	**0.86**	0.84	0.89
	XGB	0.69	0.68	0.72	0.83	0.8	0.89	**0.86**	**0.86**	0.86
	LGBM	0.69	0.68	0.75	0.78	0.76	0.81	0.81	0.81	0.81

Note: *ACC = Accuracy; Sens = Sensitivity; Spec = Specificity; LR = Logistic Regression; GBC = Gradient Boosting Classifier; XGB = Extreme Gradient Boosting; LGBM = Light Gradient Boosting Machine. Higher scores mean better classification. Bold values indicate the best-performing models for each feature subset within a given data modality.*

Table 3
Hop-level classification results by data type and feature set.

Data Type	Model	Top 10				Top 20				Top 40			
		GroupKFold-3 (ACC M(SD))	LOPOCV ACC	LOPOCV F1	LOPOCV MCC	GroupKFold-3 (ACC M(SD))	LOPOCV ACC	LOPOCV F1	LOPOCV MCC	GroupKFold-3 (ACC M(SD))	LOPOCV ACC	LOPOCV F1	LOPOCV MCC
biomecH-anical	**LR**	0.63 (0.04)	0.64	0.62	0.28	0.63 (0.04)	0.63	0.62	0.27	0.66 (0.03)	0.68	0.67	0.37
	GBC	0.71 (0.03)	0.71	0.7	0.42	0.71 (0.04)	0.73	0.73	0.46	0.70 (0.04)	0.74	0.73	0.49
	XGB	0.71 (0.03)	0.73	0.72	0.47	0.72 (0.03)	0.73	0.72	0.46	0.70 (0.03)	0.74	0.73	0.49
	LGBM	**0.70 (0.03)**	**0.75**	**0.75**	**0.51**	0.69 (0.03)	0.74	0.73	0.48	0.66 (0.03)	0.67	0.66	0.34
EMG	**LR**	0.62 (0.03)	0.63	0.61	0.26	0.62 (0.03)	0.64	0.63	0.29	0.60 (0.03)	0.62	0.6	0.24
	GBC	0.63 (0.02)	0.65	0.64	0.29	0.65 (0.03)	0.67	0.67	0.34	0.63 (0.03)	0.65	0.65	0.3
	XGB	0.62 (0.02)	0.63	0.62	0.26	**0.65 (0.03)**	**0.68**	**0.67**	**0.36**	0.63 (0.03)	0.64	0.64	0.28
	LGBM	0.63 (0.02)	0.64	0.65	0.29	0.63 (0.02)	0.66	0.66	0.32	0.61 (0.03)	0.67	0.67	0.35
Fused	**LR**	0.62 (0.03)	0.64	0.64	0.28	0.66 (0.03)	0.68	0.68	0.36	0.64 (0.03)	0.65	0.63	0.29
	GBC	0.64 (0.03)	0.67	0.66	0.34	0.72 (0.04)	0.75	0.75	0.51	0.72 (0.04)	0.77	0.76	0.54
	XGB	0.63 (0.03)	0.65	0.64	0.3	0.72 (0.03)	0.77	0.76	0.54	**0.72 (0.03)**	**0.79**	**0.78**	**0.57**
	LGBM	0.64 (0.04)	0.67	0.68	0.35	0.68 (0.04)	0.71	0.7	0.42	0.67 (0.04)	0.72	0.71	0.44

Note: *ACC = Accuracy; M(SD) = Mean (Standard Deviation); F1 = F1-Score; MCC = Matthews correlation coefficient; GroupKFold-3 = Grouped 3-fold cross-validation; LOPOCV = Leave-One-Participant-Out Cross-Validation; LR = Logistic Regression; GBC = Gradient Boosting Classifier; XGB = Extreme Gradient Boosting; LGBM = Light Gradient Boosting Machine. LOPOCV values are means across outer folds. Bold values indicate the best-performing models for each feature subset within a given data modality.*

landing biomechanics and EMG during the side-hop task. Because our study design was cross-sectional, we cannot infer directionality: self-reported fear may influence movement strategies, movement capacity may have an impact on fear, or both may co-evolve post-injury. These findings should not be interpreted as replacing questionnaire-based fear assessment with an objective metric. Instead, task-based movement assessment may complement self-reports by describing movement correlates associated with higher self-reported fear during injury-relevant tasks.

It is essential to note that these patterns were revealed using model-specific feature importance methods. Because different ML models and XAI techniques may emphasize different features, clinical interpretation should be grounded in both prior evidence and cross-model consistency. In addition to model choice, our validation strategy aimed to ensure methodological rigor. We applied LOPOCV and GroupKFold-3 to assess generalizability and performance stability. LOPOCV enabled participant-level independence, while GroupKFold-3 offered a complementary assessment across grouped samples. This dual approach limits data leakage and supports stable estimates for repeated-measures data.

Neuromuscular patterns associated with higher fear may reflect knee protective strategies, expressed as higher stiffness around the joint (Markström et al., 2022a). This may constrain adaptability in unpredictable or complex environments, potentially increasing injury risk (Bartlett et al., 2007). Additionally, sustained co-contraction can increase higher tibiofemoral compression (Tsai et al., 2012), possibly accelerating degenerative changes (Blackburn et al., 2019; Hodges et al., 2016). Clinically, addressing fear that may be associated with modified movement strategies is therefore relevant for both short-term re-injury risk (Paterno et al., 2018; Tagesson and Kvist, 2015) and long-term knee health (Blackburn et al., 2019; Hodges et al., 2016).

Pelvic obliquity was identified by the QDA model as an influential variable for fear classification (Ore et al., 2020). This variable describes the pelvis tilt in the frontal plane. A previous review of hip-focused exercises (Ford et al., 2015) has found such interventions to reduce dynamic lower extremity valgus, thus indicating a meaningful role of pelvic movement for lower limb injuries. Additionally, females with dynamic knee valgus and patellofemoral pain showed increased pelvic obliquity with lateral tilt of the pelvis towards the weight-bearing limb (i.e., pelvic hike) during single-leg squats with a corrected technique compared with their normal technique (Graci and Salsich, 2015). While knee valgus is critical to assess, being associated with poor knee control and ACL injury risk (Hewett et al., 2005; Padua et al., 2012), we did not find any related top-ranked features in our models. A possible explanation is our choice of sagittal-control muscle activations, while dynamic knee valgus has been associated more with hip abductor activation (Bittencourt et al., 2012).

Muscular imbalance between knee flexors and extensors is commonly considered a risk factor for re-injury, although limited evidence warrants better monitoring (Kellis et al., 2023). It is thus relevant to further develop clinical tools for analyzing muscular activation patterns and detect abnormalities associated with increased injury risk. Wearable IMU or EMG systems combined with purposeful ML tools could enable tailored interventions to address fear of re-injury early in rehabilitation. Incorporating objective assessment of biomechanical and neuromuscular movement characteristics associated with fear of re-injury into return-to-play testing alongside traditional metrics would improve the identification of fearful individuals potentially at higher risk of re-injury prior to resuming high demanding sports (Cronström et al., 2023). Our study also demonstrates the value of integrating multimodal data with advanced ML techniques to improve screening of non-injured athletes as well as monitoring of injured individuals continuously across rehabilitation and after returning to sport. Such efforts may increase therapeutic precision in understanding when to provide suitable treatment options for individuals with high fear, such as e.g., cognitive behavioral therapy (Coronado et al., 2020).

We evaluated ten classifiers from linear, discriminant, distance-based, and ensemble tree families (Halilaj et al., 2018; James et al., 2013). We highlight models that were both interpretable and consistently competitive under LOPOCV and GroupKFold-3. Overall, the strongest and most stable performance was observed for gradient-boosted tree models in the fused dataset (participant level: up to 0.86 accuracy with XGB/GBC; Table 2; hop level: 0.79 LOPOCV accuracy with XGB using the top 40 features; Table 3). For full accuracy heatmaps across feature counts and all algorithms, see Supplementary S3. Support Vector Machine (SVM) and neural networks were not included in the final model set due to higher tuning demands and no clear performance gain in preliminary comparisons. Larger cohorts may warrant revisiting these families.

The best hop-level setting (fused XGB, top 40 features) achieved 0.79 accuracy under LOPOCV, indicating non-trivial trial-level misclassification (Table 3). To clarify whether errors are balanced, participant-level sensitivity and specificity were reported (Table 2). For the best fused participant-level model (XGB, top 40), sensitivity and specificity were similar (0.86 and 0.86, respectively), suggesting no strong skew toward false positives or false negatives. We view the model output as a complement to, rather than replacement for questionnaire-based assessment. Future work should test its prospective clinical utility and external validity.

In rehabilitation settings, our approach could be applied during side hop testing to provide a task-based movement profile associated with higher self-reported fear status. The side hop also challenges knee control more than other common clinical tests such as hops for distance or

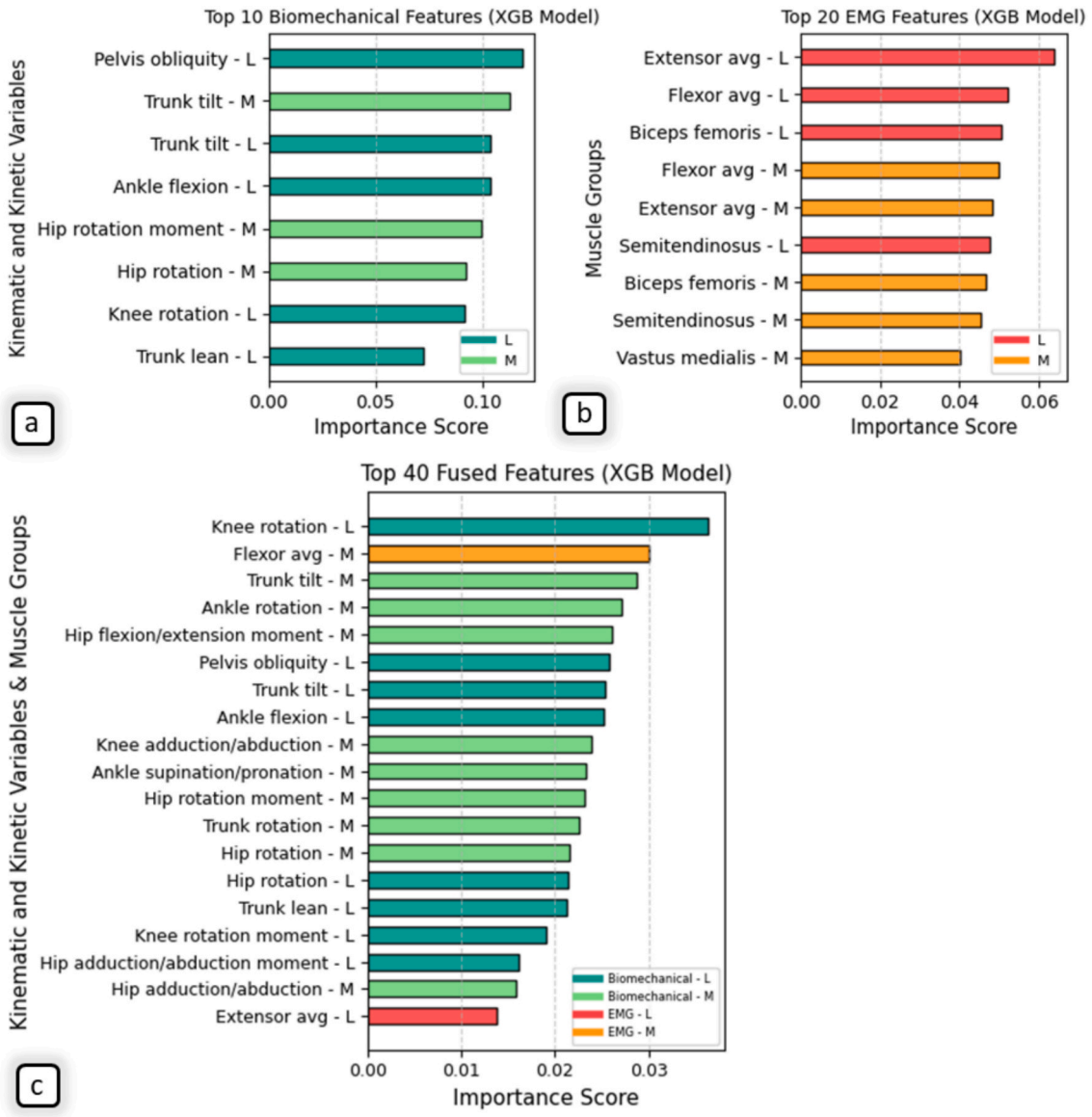

Fig. 3. Variable-level summary of the top-ranked tsfresh features used in the best-performing XGB configurations (features ranked using the GBC importance scores). Panels show (a) biomechanical: Top-10 ranked features, summarized by underlying variable class and landing side; (b) EMG: Top-20 ranked features, summarized by muscle and landing side; (c) fused: Top-40 ranked features, summarized by variable class and side. For interpretability, multiple ranked tsfresh features that originate from the same underlying variable may be grouped, so fewer than N unique plotted labels can appear. The complete (variable × tsfresh-feature) rankings are reported in Supplementary Material S4. ***Note:*** *Flexor avg and Extensor avg refer to the time-normalized average of root mean square (RMS) EMG activity over the landing phase, as defined in the Methods (Engineered EMG Variables).*

height (Markström et al., 2023). For wider implementation, portable sensing options (e.g., EMG, IMUs, and marker less video-based systems) require task-specific validation. When IMUs are used to estimate joint kinematics/kinetics, frontal-plane quantities can be less accurate than sagittal-plane estimates relative to optical systems (Dahl et al., 2020), which is particularly relevant for valgus-related movement patterns. However, IMUs also provide rich raw acceleration and angular-velocity signals that may support classification without explicitly reconstructing joint kinematics/kinetics. Future work should evaluate this.

5.2. Limitations

First, fear labels were derived from a single self-report item (TSK-17, Q9), which under competitive contexts (Grossbard et al., 2007) may be prone to under-reporting. Collecting ratings outside sport-specific pressure likely mitigated this, but clinician-rated or multi-item measures could strengthen ground truth. Second, our cross-sectional design precludes inferences about directionality between self-reported fear and movement patterns and about how these features change over time. Longitudinal designs could verify whether changes in trunk tilt or knee rotation track fear trajectories. Third, we tuned hyper-parameters on the biomechanical dataset and reused them for EMG and fused models. This cut computation but may have reduced EMG accuracy. Per-modality tuning could improve performance. Fourth, we evaluated group differences and model performance using the SRSH task only. Fear-associated biomechanics and EMG patterns may differ across movement tasks and according to biological sex. Future work should compare SRSH with other standardized functional paradigms to test task-dependence directly and address possible sex-related differences, which was outside the current scope.

6. Conclusion

This study demonstrates that machine learning models can classify fear of re-injury after ACLR with very high accuracy, using EMG-derived features alone and additional improvements in a multimodal approach integrating biomechanical data. Future implementations of these methods, also using wearable EMG and/or IMU systems, may support clinicians in identifying fearful individuals who may benefit from a more comprehensive rehabilitation approach targeting psychological barriers to return to sports or physical activity.

CRediT authorship contribution statement

Abdolamir Karbalaie: Writing – review & editing, Writing – original draft, Visualization, Software, Methodology, Investigation, Formal analysis, Conceptualization. **Adam Grinberg:** Writing – review & editing, Investigation, Data curation. **Andrew Strong:** Writing – review & editing, Investigation, Data curation. **Helena Grip:** Writing – review & editing, Investigation. **Kalle Prorok:** Writing – review & editing, Validation, Investigation. **Charlotte K. Häger:** Writing – review & editing, Supervision, Resources, Project administration, Methodology, Investigation, Funding acquisition, Data curation, Conceptualization. **Tomas Nordström:** Writing – review & editing, Validation, Supervision, Methodology, Conceptualization.

Funding

CK Häger obtained the following funding for the research for the current study: the Swedish Research Council (Grant No. K2014-99X-21876-04-4; 2017-00892; 2022-00774), Region Västerbotten (Grant No. ALF VLL548501, VLL838421 and Strategic funding VLL-358901; Project No. 7002795; Cutting Edge funding RV966109 and 2022-2024; ALF funding RV 967112 and 2022-2024), the Swedish Research Council for Sports Science (Grants No.; 2021/9 P2022; 2022/10; P2023-003; P2024-0036; P2025-0069), Umeå University School of Sport Science (Grant No IH 5.2–25-2021; IH 5.1-7-2025 Karbalaie), and King Gustaf V and Queen Victoria's Foundation of Freemasons.

Declaration of competing interest

The authors declare that they have no known competing financial interests or personal relationships that could have appeared to influence the work reported in this paper.

Acknowledgements

We thank all the study participants for their effort and dedication. We would also like to acknowledge Jonas Selling for technical support.

Appendix A. Supplementary data

Supplementary data to this article can be found online at https://doi.org/10.1016/j.jbiomech.2026.113346.

References

Ardern, C.L., Webster, K.E., Taylor, N.F., Feller, J.A., 2011. Return to sport following anterior cruciate ligament reconstruction surgery: a systematic review and meta-analysis of the state of play. Br. J. Sports Med. 45, 596–606.

Ardern, C.L., Taylor, N.F., Feller, J.A., Webster, K.E., 2014. Fifty-five per cent return to competitive sport following anterior cruciate ligament reconstruction surgery: an updated systematic review and meta-analysis including aspects of physical functioning and contextual factors. Br. J. Sports Med. 48, 1543–1552.

Baez, S., Cormier, M., Andreatta, R., Gribble, P., Hoch, J.M., 2021. Implementation of In vivo exposure therapy to decrease injury-related fear in females with a history of ACL-Reconstruction: A pilot study. Physical Therapy in Sport.

Bartlett, R., Wheat, J., Robins, M., 2007. Is movement variability important for sports biomechanists? Sports Biomech. 6, 224–243.

Bittencourt, N.F., Ocarino, J.M., Mendonça, L.D., Hewett, T.E., Fonseca, S.T., 2012. Foot and Hip Contributions to High Frontal Plane Knee Projection Angle in Athletes: a Classification and Regression Tree Approach. Journal of Orthopaedic & Sports Physical Therapy 42, 996–1004.

Blackburn, T., Pietrosimone, B., Goodwin, J.S., Johnston, C., Spang, J.T., 2019. Co-activation during gait following anterior cruciate ligament reconstruction. Clin. Biomech. 67, 153–159.

Christ, M., Braun, N., Neuffer, J., Kempa-Liehr, A.W., 2018. Time Series FeatuRe Extraction on basis of Scalable Hypothesis tests (tsfresh - A Python package). Neurocomputing 307, 72–77.

Coronado, R.A., Sterling, E.K., Fenster, D.E., Bird, M.L., Heritage, A.J., Woosley, V.L., Burston, A.M., Henry, A.L., Huston, L.J., Vanston, S.W., 2020. Cognitive-behavioral-based physical therapy to enhance return to sport after anterior cruciate ligament reconstruction: an open pilot study. Phys. Ther. Sport 42, 82–90.

Cronström, A., Tengman, E., Häger, C.K., 2023. Return to sports: a risky business? A systematic review with meta-analysis of risk factors for graft rupture following ACL reconstruction. Sports Med. 53, 91–110.

Dahl, K.D., Dunford, K.M., Wilson, S.A., Turnbull, T.L., Tashman, S., 2020. Wearable sensor validation of sports-related movements for the lower extremity and trunk. Med. Eng. Phys. 84, 144–150.

Dekking, F.M., Kraaikamp, C., Lopuhaä, H.P., Meester, L.E., 2005. A Modern Introduction to Probability and Statistics. Springer-Verlag, London.

Dudley, R.I., Lohman, E.B., Patterson, C.S., Knox, K.G., Gharibvand, L., 2022. The relationship between kinesiophobia and biomechanics in anterior cruciate ligament reconstructed females. Phys. Ther. Sport 56, 32–37.

Du, T., Shi, Y., Huang, H., Liang, W., Miao, D., 2022. Current study on the influence of psychological factors on returning to sports after ACLR. Heliyon 8, e12434.

Ford, K.R., Nguyen, A.D., Dischiavi, S.L., Hegedus, E.J., Zuk, E.F., Taylor, J.B., 2015. An evidence-based review of hip-focused neuromuscular exercise interventions to address dynamic lower extremity valgus. Open Access J. Sports Med. 6, 291–303.

Graci, V., Salsich, G.B., 2015. Trunk and lower extremity segment kinematics and their relationship to pain following movement instruction during a single-leg squat in females with dynamic knee valgus and patellofemoral pain. J. Sci. Med. Sport 18, 343–347.

Grossbard, J.R., Cumming, S.P., Standage, M., Smith, R.E., Smoll, F.L., 2007. Social desirability and relations between goal orientations and competitive trait anxiety in young athletes. Psychol. Sport Exerc. 8, 491–505.

Guyon, I., E.a.,, 2003. An introduction to variable and feature selection. The Journal of Machine Learning Research 3, 25.

Halilaj, E., Rajagopal, A., Fiterau, M., Hicks, J.L., Hastie, T.J., Delp, S.L., 2018. Machine learning in human movement biomechanics: best practices, common pitfalls, and new opportunities. J. Biomech. 81, 1–11.

Hamdan, M., Haddad, B.I., Amireh, S., Abdel Rahman, A.M.A., Almajali, H., Mesmar, H., Naum, C., Alqawasmi, M.S., Albandi, A.M., Alshrouf, M.A., 2025. Reasons why patients do not return to sport post ACLReconstruction: A cross-sectional study. J. Multidiscip. Healthc. 18, 329–338.

Heil, J., 2000. The injured athlete. Emotions in Sport 245–265.

Hermens, H.J., Freriks, B., Merletti, R., Stegeman, D.F., Blok, J.H., Rau, G., Disselhorst-Klug, C., Hägg, G., 1999 European recommendations for surface electromyography: Results of the SENIAM Project. Chapter 8. Roessingh Research and Development b.v. (RRD), Enschede, the Netherlands.

Hewett, T.E., Myer, G.D., Ford, K.R., Heidt, R.S., Colosimo, A.J., McLean, S.G., van den Bogert, A.J., Paterno, M.V., Succop, P., 2005. Biomechanical measures of neuromuscular control and valgus loading of the knee predict anterior cruciate ligament injury risk in female athletes: a prospective study. Am. J. Sports Med. 33, 492–501.

Hodges, P.W., van den Hoorn, W., Wrigley, T.V., Hinman, R.S., Bowles, K.-A., Cicuttini, F., Wang, Y., Bennell, K., 2016. Increased duration of co-contraction of medial knee muscles is associated with greater progression of knee osteoarthritis. Man. Ther. 21, 151–158.

James, G., Witten, D., Hastie, T., Tibshirani, R., 2013. An introduction to statistical learning: with applications in R. Springer.

Johnson, W.R., Mian, A., Lloyd, D.G., Alderson, J.A., 2019. On-field player workload exposure and knee injury risk monitoring via deep learning. J. Biomech. 93, 185–193.

Karbalaie, A., Strong, A., Nordström, T., Schelin, L., Selling, J., Grip, H., Prorok, K., Häger, C.K., 2025. Beyond self-reports after anterior cruciate ligament injury – machine learning methods for classifying and identifying movement patterns related to fear of re-injury. J. Sports Sci. 1–15.

Kellis, E., Sahinis, C., Baltzopoulos, V., 2023. Is hamstrings-to-quadriceps torque ratio useful for predicting anterior cruciate ligament and hamstring injuries? a systematic and critical review. J. Sport Health Sci. 12, 343–358.

King, M.F., Bruner, G.C., 2000. Social desirability bias: a neglected aspect of validity testing. Psychol. Mark. 17, 79–103.

Krishnakumar, S., van Beijnum, B.-J.-F., Baten, C.T., Veltink, P.H., Buurke, J.H., 2024. Estimation of kinetics using IMUs to monitor and aid in clinical decision-making during ACL rehabilitation: a systematic review. Sensors 24, 2163.

Lee, G., Lee, S., 2024. Deep-learning domain adaptation to improve generalizability across subjects and contexts in detecting construction workers' stress from biosignals. J. Comput. Civ. Eng. 38.

Markström, J.L., Schelin, L., Häger, C.K., 2021. A novel standardised side hop test reliably evaluates landing mechanics for anterior cruciate ligament reconstructed persons and controls. Sports biomechanics.

Markström, J.L., Grinberg, A., Häger, C.K., 2022a. Fear of re-injury following anterior cruciate ligament reconstruction is manifested in muscle activation patterns of single-leg side-hop landings. Phys. Ther.

Markström, J.L., Liebermann, D.G., Schelin, L., Häger, C.K., 2022b. Atypical lower limb mechanics during weight acceptance of stair descent at different time frames after anterior cruciate ligament reconstruction. Am. J. Sports Med. 03635465221095236.
Markström, J.L., Tengman, E., Häger, C.K., 2023. Side-hops challenge knee control in the frontal and transversal plane more than hops for distance or height among ACL-reconstructed individuals. Sports Biomech. 22, 142–159.
Moghadam, S.M., Yeung, T., Choisne, J., 2023. A comparison of machine learning models' accuracy in predicting lower-limb joints' kinematics, kinetics, and muscle forces from wearable sensors. Sci. Rep. 13, 5046.
Ore, V., Nasic, S., Riad, J., 2020. Lower extremity range of motion and alignment: a reliability and concurrent validity study of goniometric and three-dimensional motion analysis measurement. Heliyon 6, e04713.
Padua, D.A., Bell, D.R., Clark, M.A., 2012. Neuromuscular characteristics of individuals displaying excessive medial knee displacement. J. Athl. Train. 47, 525–536.
Palma Fraga, R., Kang, Z., Axthelm, C.M., 2023. Effect of machine learning cross-validation algorithms considering human participants and time-series: Application on biometric data obtained from a virtual reality experiment. Proc. Hum. Factors Ergon. Soc. Annu. Meet. 67, 2162–2167.
Paterno, M.V., Flynn, K., Thomas, S., Schmitt, L.C., 2018. Self-reported fear predicts functional performance and second ACL injury after ACL reconstruction and return to sport: a pilot study. J Sports Health 10, 228–233.
Saeys, Y., Inza, I., Larranaga, P., 2007. A review of feature selection techniques in bioinformatics. Bioinformatics 23, 2507–2517.
Schwartz, M.H., Rozumalski, A., 2005. A new method for estimating joint parameters from motion data. J. Biomech. 38, 107–116.
Tagesson, S., Kvist, J., 2015. Greater fear of re-injury and increased tibial translation in patients who later sustain an ACL graft rupture or a contralateral ACL rupture: A pilot study. J. Sports Sci. 1–8.
Trigsted, S.M., Cook, D.B., Pickett, K.A., Cadmus-Bertram, L., Dunn, W.R., Bell, D.R., 2018. Greater fear of reinjury is related to stiffened jump-landing biomechanics and muscle activation in women after ACL reconstruction. Knee Surg. Sports Traumatol. Arthrosc. 26, 3682–3689.
Tsai, L.C., McLean, S., Colletti, P.M., Powers, C., 2012. Greater Muscle Co-Contraction Results in Increased Tibiofemoral Compressive Forces in Females Who Have Undergone Anterior Cruciate Ligament Reconstruction. J. Orthop. Res. 30, 2007–2014.
Wiechman, S.A., Smith, R.E., Smoll, F.L., Ptacek, J., 2000. Masking effects of social desirability response set on relations between psychosocial factors and sport injuries: A methodological note. J. Sci. Med. Sport 3, 194–202.
Woods, M.P., Asmundson, G.J., 2008. Evaluating the efficacy of graded in vivo exposure for the treatment of fear in patients with chronic back pain: A randomized controlled clinical trial. Pain 136, 271–280.